

OPEN

# Head motion predictability explains activity-dependent suppression of vestibular balance control

H. Dietrich<sup>1,5</sup>, F. Heidger<sup>2,5</sup>, R. Schniepp<sup>1,2</sup>, P. R. MacNeilage<sup>1,3</sup>, S. Glasauer<sup>1,4</sup> & M. Wuehr<sup>1\*</sup>

Vestibular balance control is dynamically weighted during locomotion. This might result from a selective suppression of vestibular inputs in favor of a feed-forward balance regulation based on locomotor efference copies. The feasibility of such a feed-forward mechanism should however critically depend on the predictability of head movements (HMP) during locomotion. To test this, we studied in 10 healthy subjects the differential impact of a stochastic vestibular stimulation (SVS) on body sway (center-of-pressure, COP) during standing and walking at different speeds and compared it to activity-dependent changes in HMP. SVS-COP coupling was determined by correlation analysis in frequency and time domains. HMP was quantified as the proportion of head motion variance that can be explained by the average head trajectory across the locomotor cycle. SVS-COP coupling decreased from standing to walking and further dropped with faster locomotion. Correspondingly, HMP increased with faster locomotion. Furthermore, SVS-COP coupling depended on the gait-cycle-phase with peaks corresponding to periods of least HMP. These findings support the assumption that during stereotyped human self-motion, locomotor efference copies selectively replace vestibular cues, similar to what was previously observed in animal models.

The vestibular system encodes head orientation and motion to facilitate balance reflexes that ensure postural equilibrium during passive as well as self-initiated movements<sup>1</sup>. During locomotion, i.e., stereotyped self-motion, vestibular influences on balance control appear to be dynamically up- or down-regulated in dependence on the phase and speed of the locomotor pattern. Accordingly, vestibulospinal reflexes exhibit phasic modulations across the locomotor cycle<sup>2,3</sup> with the result that balance is particularly sensitive to vestibular perturbations at specific phases of the gait cycle<sup>4</sup>. Furthermore, vestibular influences appear to be down-weighted during faster locomotion. Accordingly, the destabilizing impact of a vestibular loss or perturbation on the gait pattern decreases with increasing locomotion speeds<sup>5–9</sup>.

It was previously assumed that activity-dependent modulations of vestibular balance reflexes might reflect an up- or down-regulation of a concurrent intrinsic feed-forward control of posture<sup>10–13</sup>. Accordingly, balance adjustments during self-motion might not solely rely on sensory feedback about how the body has moved, but also on predictions of resultant movements derived from efference copies of the motor command<sup>14</sup>. Physiological evidence for such a direct feed-forward control mode has recently been shown for animal locomotion. During *Xenopus laevis* tadpole swimming, intrinsic efference copies of the locomotor command deriving from spinal central pattern generators (CPG) were shown to directly trigger ocular adjustments for gaze stabilization and selectively cancel out any afferent (ex- and reafferent) vestibular inputs<sup>10,15</sup>. Thus, also during human stereotyped locomotion, efference copies might provide estimates of resultant head motion and assist or even substitute vestibular feedback cues in gaze and balance regulation. The feasibility of such a direct feed-forward mechanism should however critically rely on the predictability or stereotypy of head movements during locomotion<sup>16</sup>.

Following this intuition, a statistically optimal model was recently proposed, that relates an empirically quantified metric (i.e., the kinematic predictability metric) of head motion predictability to the relative weighting of vestibular vs. motor efference copy cues in gaze and balance regulation during locomotion<sup>12</sup>. According to the model, activities linked to less stereotyped head movements should be more dependent on vestibular cues than

<sup>1</sup>German Center for Vertigo and Balance Disorders, University Hospital, LMU, Munich, Germany. <sup>2</sup>Department of Neurology, University Hospital, LMU, Munich, Germany. <sup>3</sup>Department of Psychology, Cognitive and Brain Sciences, University of Nevada, Nevada, USA. <sup>4</sup>Institute of Medical Technology, Brandenburg University of Technology Cottbus-Senftenberg, Senftenberg, Germany. <sup>5</sup>These authors contributed equally: H. Dietrich and F. Heidger. \*email: [Max.Wuehr@med.uni-muenchen.de](mailto:Max.Wuehr@med.uni-muenchen.de)

activities with highly predictable head motion patterns. Likewise, timepoints during the stride cycle when head movement is less stereotyped should exhibit more vestibular dependence. To assess this hypothesis, we examined whether activity-dependent modulations of vestibular balance reflexes can be explained by alterations in the predictability of head movements. Modulations in vestibular balance control during different activities, i.e., standing as well as slow or faster walking, were studied by analyzing the differential impact of a continuous stochastic vestibular stimulation (SVS) on body sway (i.e., center-of-pressure-displacements, COP) in the frequency (coherence) and time (cross-correlation, phase) domain. In parallel, we quantified the predictability of head kinematics associated with these activities and related this metric to an estimate of relative sensory weight.

Using this theoretical and evidence-based approach we aimed to evaluate three hypotheses concerning the role of vestibular cues in balance regulation: (1) Compared to quiet standing, vestibular influence on balance control should decrease during walking due to the presence of a locomotor efference copy; (2) it should be further down-regulated with faster locomotion due to increasingly stereotyped head kinematics during faster locomotion; (3) phasic modulations of vestibular balance reflexes across the gait cycle should correspond to phase-dependent alterations in head motion predictability.

## Methods

**Subjects.** Ten healthy subjects (mean age  $29.3 \pm 3.7$  years, 3 females) participated in the study. None of the participants reported any auditory, vestibular, neurologic, cardio-vascular or orthopedic disorders. All subjects had normal or corrected-to-normal vision. Each participant gave written informed consent prior to the experiments. The Ethics Committee of the University of Munich approved the study protocol, which was conducted in conformity with the Declaration of Helsinki.

**Galvanic vestibular stimulation.** Galvanic vestibular stimulation uses the external application of electrical current to modulate semicircular canal and otolith afferent activity in the vestibular endorgans<sup>17–19</sup>. A pair of conductive rubber electrodes was attached bilaterally over the left and right mastoid process behind the ears. A stochastic galvanic vestibular stimulation (SVS) delivered via this electrode configuration with the head facing forward primarily elicits a postural roll response in the frontal plane<sup>20,21</sup>. Before electrode placement, the skin surface at the electrode sites was cleaned and dried, and a layer of electrode gel was applied before electrode placing to achieve uniform current density and minimize irritation to the skin during stimulation. The SVS profile consisted of a bandwidth-limited stochastic stimulus (frequency range: 0–25 Hz, peak amplitude  $\pm 4.5$  mA, root mean square (RMS) 1.05 mA) delivered via a constant-current stimulator (Model DS5, Digitimer, Hertfordshire, UK). The stimulus bandwidth (0–25 Hz) was chosen to cover the entire frequency response bandwidth of vestibular-induced modulations in lower limb muscle activity<sup>2,3</sup>.

**Test procedures.** Each participant stood and walked on a pressure-sensitive treadmill (Zebris®, Isny, Germany; h/p/cosmos®, Nussdorf-Traunstein, Germany; 1.6 m long; sampling rate of 100 Hz). Five different conditions were tested in randomized order: three stimulation conditions with continuous SVS and two non-stimulation conditions. SVS was presented during 180 s of quiet standing, as well as during slow walking at 0.4 m/s and medium walking at 0.8 m/s, each for 600 s. Head movements without SVS stimulation were recorded during walking at 0.4 and 0.8 m/s, each for 300 s. Walking was guided by a metronome with a cadence of 52 steps/min for the slow and 78 steps/min for the medium walking speed, respectively. Walking speeds and cadences were chosen in order to allow direct comparison with previous studies<sup>2,3,22</sup>. During trials, participants were instructed to fixate on a target located 3 m in front of them at eye level. Before each recording, participants were given 30 s to acclimatize to the preset treadmill speed and walking cadence. Between trials, participants were given at least two minutes to recover.

**Data analysis.** *Center-of-pressure displacements, head kinematics, and gait parameters.* For each stance and walking trial, the continuous trajectory of the center-of-pressure (COP) was computed as the weighted average of the pressure data recorded from the treadmill by using the standard method for determining the barycenter ( $\text{sum of mass} \times \text{position} / \text{sum of mass}$ )<sup>23</sup>. COP motion was analyzed in the medio-lateral (ML) dimension, i.e., the primary dimension of postural responses induced by binaural bipolar SVS<sup>20</sup>. Head kinematics in ML dimension (i.e., linear head acceleration in the ML dimension and angular head velocity in the roll plane) were measured with an inertial measurement unit (IMU) containing a triaxial accelerometer and gyroscope (APDM, Inc., Portland, OR, sampling rate of 128 Hz), strapped to the forehead. Furthermore, for each walking trial, the following spatiotemporal gait parameters were analyzed: base of support, stride length, stride time, single support percentage, and double support percentage, as well as the coefficient of variation (CV) of each of these parameters.

*Cross-correlation and coherence analysis.* For all stimulation trials, correlation analysis in the frequency (coherence) and time (cross-correlation, phase) domain was used to estimate the average SVS-induced variations in COP-displacements. Analysis was performed for the first 180 s of each recording to yield an equal amount of analyzed data points for the stance and walking trials. Since coherence is normalized by the power in both SVS- and COP-signals, it is particularly suitable to compare SVS-COP coupling across different activities that are linked to different magnitudes of COP-displacements. Coherence estimates with confidence limits were computed based on the auto-spectra of the SVS and COP signals ( $P_{AA}(f)$  and  $P_{BB}(f)$  respectively) as well as the cross-spectrum ( $P_{AB}(f)$ ) using a finite fast Fourier transform with a block size of 2 s resulting in a frequency resolution of 0.5 Hz<sup>24</sup>.

$$C_{AB}(f) = \frac{|P_{AB}(f)|}{P_{AA}(f)P_{BB}(f)}$$

This yielded a 95% confidence limit for coherence estimates of 0.033<sup>24</sup>. The resultant coherence estimate is a unitless measure bounded between 1 (indicating a perfect linear relationship at the absence of noise) and 0 (indicating independence between the two signals).

Cross-correlations between SVS and COP signals were computed to determine the onset and peak of SVS-induced COP displacements. For this purpose, the inverse Fourier transform of the cross-spectrum  $P_{AB}(f)$  was computed and normalized by the norm of the input and output vectors to obtain unitless correlation values bounded between  $-1$  and  $1$ <sup>2</sup>. The resultant 95% confidence limit for cross-correlation estimates was 0.015. Finally, phase estimates between the SVS and COP signals were estimated from the complex valued coherence function. This allows to determine the phase lag corresponding to frequency bandwidths with significant SVS-COP coherence estimates<sup>25</sup>. The slope of the phase values over the range of significant coherence estimates was computed using regression analysis and multiplied by  $1000/2\pi$  to yield an estimate of the phase lag in milliseconds.

For the two walking stimulation trials, we further analyzed phasic modulations in the correlation between SVS and COP signals across the average gait cycle, using time-dependent coherence analysis according to a previously described procedure<sup>2,3</sup>. First SVS and COP signals were cut into individual strides synchronized to the left heel strike and then time-normalized by resampling each stride to a total of 300 samples. The first 250 strides of each trial were taken for further analysis and padded at the start and end with data from the previous and subsequent strides to avoid distortions in the subsequent correlation analysis. Time-dependent coherence was then estimated using a Morlet wavelet decomposition based on the method of Zhan *et al.*<sup>26</sup>, with a resultant frequency resolution of 0.5 Hz and 95% confidence limits of 0.018.

**Head motion predictability.** Head motion predictability (HMP) was quantified separately for linear head acceleration and angular head velocity recorded during the non-stimulation conditions according to a previously proposed procedure<sup>12</sup>. First, IMU signals were cut into individual strides synchronized to the left heel strike and further time-normalized by resampling each stride to a total of 300 samples. Head motion data from the first 125 strides ( $N = 125$ ) was used for further analysis and averaged to reconstruct the mean head motion trajectory across the stride cycle, i.e., the stride-cycle attractor. Subsequently, the total variance  $SS_{tot}$  and residual variance  $SS_{res}$  of head motion were calculated:

$$SS(t)_{tot} = \frac{1}{N} \sum_{i=1}^N (h(t)_i - \bar{h})^2$$

$$SS(t)_{res} = \frac{1}{N} \sum_{i=1}^N (h(t)_i - f(t))^2$$

where  $h(t)_i$  is the head motion during the  $i$  th stride at the normalized stride time  $t$ ,  $\bar{h}$  is the average head motion over all stride cycle phases and strides, and  $f(t)$  denotes the stride cycle attractor. Correspondingly,  $SS_{tot}$  quantifies the signal deviation from the overall mean signal whereas  $SS_{res}$  gives the signal deviation from the stride cycle attractor.

Using these metrics, the proportion of head motion variance that can be explained by the stride cycle attractor, i.e., explained variance ( $V_{exp} = 1 - SS_{res}/SS_{tot}$ ), and the proportion of residual head motion variance  $V_{res} = SS_{res}/SS_{tot}$  can be derived. Low values of  $V_{res}$  indicate a high HMP. Hence, knowing the exact stride cycle phase, feed-forward signals of the locomotor command can provide reliable information about the most likely ongoing movement. However, as  $V_{res}$  increases, head motion prediction based on stride cycle phase information becomes less accurate and additional sensory cues are required for head motion estimation. These considerations can be expressed in the form of a statistically optimal model (in the sense of obtaining the lowest-variance estimate), i.e., the maximum likelihood estimation model for cue integration<sup>27</sup>. Accordingly, head motion  $\hat{H}$  can be estimated by a weighted linear combination of vestibular (sensory,  $S$ ) and efference copy (motor,  $M$ ) cues with weights  $w_{sens}$  and  $w_{mot}$  corresponding to the relative reliability of these cues:

$$\hat{H} = w_{sens}S + w_{mot}M$$

$$w_{sens} = \frac{\sigma_{mot}^2}{\sigma_{sens}^2 + \sigma_{mot}^2} \quad w_{mot} = \frac{\sigma_{sens}^2}{\sigma_{sens}^2 + \sigma_{mot}^2}$$

The above weights can now be estimated using the head motion data based on the following two assumptions: (1) According to Weber's law, sensory noise is assumed to be signal-dependent, i.e., its variance should be proportional to the squared signal<sup>28</sup>. As the average signal is approximately zero for oscillatory locomotor movements, sensory noise can be estimated by  $\sigma_{sens}^2 = kSS_{tot}$ , with the Weber's fraction  $k$ . (2) If the intended head motion during each stride equals the stride cycle attractor, motor noise can be estimated as  $\sigma_{mot}^2 = SS_{res}$ . According to Fitt's law, motor noise is assumed to increase with faster movement velocities<sup>29-31</sup>. Note, that this estimate of  $\sigma_{mot}^2$  represents an upper limit of motor noise since in this estimate any deviation from the gait cycle attractor including intentional deviations (e.g. head turns) are interpreted as motor noise. Thus, the actual motor noise is likely to

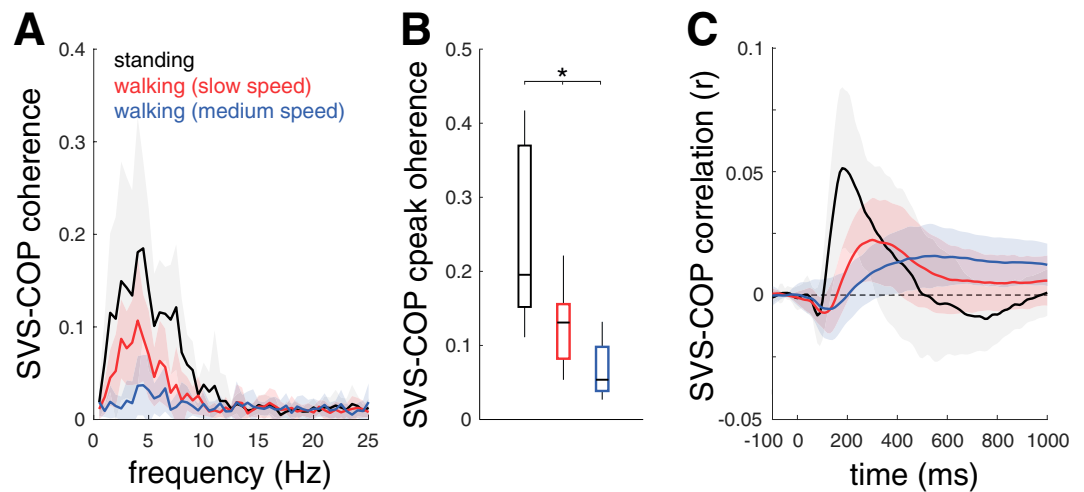


**Figure 1.** Correlation analysis in frequency and time domain for coupling between SVS and COP displacements during different activities. **(A)** Coherence functions, **(B)** peak coherence values, and **(C)** corresponding cross-correlations between SVS and COP displacements. SVS-COP coherence drops from standing to slow walking and is further reduced at faster walking speed. SVS-induced COP displacements exhibit a short latency response around 80–120 ms and a medium latency response of opposite polarity at around 200–290 ms. \*Indicates a significant difference. SVS: *stochastic vestibular stimulation*; COP: *center-of-pressure*.

be lower than this estimate. Based on these assumptions, sensory weight can be expressed as directly proportional to  $V_{res}$ :

$$w_{sens} = \frac{SS_{res}}{k * SS_{tot} + SS_{res}} * \frac{1/SS_{tot}}{1/SS_{tot}} = \frac{V_{res}}{V_{res} + k}$$

**Statistical analysis.** Data are reported as mean  $\pm$  SD. The effects of correlation analysis parameters, head predictability estimates, and gait parameters were analyzed using a repeated-measures analysis of variance (rmANOVA) and Bonferroni post hoc analysis with condition (standing, slow and medium walking) as factor. Results were considered significant if  $p < 0.05$ . Statistical analysis was performed using SPSS (Version 25.0; IBM Corp., Armonk, NY).

## Results

All participants exhibited significant correlations between SVS and COP displacements in both the frequency and time domain. SVS-COP overall coherence within the 0–25 Hz bandwidth peaked at  $4.8 \pm 1.4$  Hz for standing (COP RMS:  $10.9 \pm 7.4$  mm),  $3.9 \pm 0.8$  Hz for slow (COP RMS:  $62.6 \pm 8.6$  mm), and  $4.6 \pm 2.4$  Hz for medium (COP RMS:  $60.7 \pm 10.8$  mm) walking speed ( $F_{2,18} = 1.2$ ;  $p = 0.526$ ; Fig. 1A). Peak coherence dropped from standing to slow walking and further decreased with faster walking ( $F_{2,18} = 22.6$ ;  $p < 0.001$ ; Fig. 1B). Cross-correlation analysis revealed a short latency component of SVS-induced COP responses at  $85 \pm 11$  ms for standing and slightly later responses for slow ( $112 \pm 12$  ms) and medium ( $111 \pm 9$  ms) walking speeds ( $F_{2,18} = 54.1$ ;  $p < 0.001$ ). A medium latency response of opposite polarity occurred at  $203 \pm 45$  ms for standing and slightly later for slow ( $273 \pm 18$  ms) and medium ( $273 \pm 25$  ms) walking speeds ( $F_{2,18} = 21.7$ ;  $p = 0.001$ ; Fig. 1C). Phase lags at frequency bandwidth with significant coherence estimates corresponded to the medium latency response with  $204 \pm 44$  ms for standing, and  $267 \pm 21$  ms for slow, and  $275 \pm 22$  ms for medium walking speed ( $F_{2,18} = 24.0$ ;  $p < 0.001$ ).

Similar to global coherence estimates, time-frequency analysis of SVS-COP coupling across the gait cycle revealed a drop of peak coherence from slow to medium walking speed ( $F_{1,9} = 15.5$ ;  $p < 0.001$ , Fig. 2A–C). Analysis of HMP revealed a corresponding decrease in mean head motion  $V_{res}$  (i.e., an increase in HMP) from slow to medium walking speed for both linear head acceleration and angular head velocity ( $F_{1,18} = 14.0$ ;  $p = 0.001$ , Fig. 2A–C). Furthermore, HMP was generally higher for linear head acceleration compared to angular head velocity ( $F_{1,18} = 44.7$ ;  $p < 0.001$ , Fig. 2C). SVS-COP coupling across the gait cycle exhibited phasic modulations with two distinct peaks occurring at  $25.0 \pm 2.4\%$  and  $74.3 \pm 2.7\%$  of the gait cycle during slow walking and at  $25.4 \pm 1.4\%$  and  $76.6 \pm 1.4\%$  of the gait cycle during walking at medium speed (Fig. 2A,B). In accordance, the estimated HMP was similarly modulated throughout the gait cycle. Periods of maximum  $V_{res}$  (i.e., least predictability) of angular head velocity corresponded to peaks of SVS-COP coherence (at  $21.6 \pm 2.8\%$  and  $73.5 \pm 3.1\%$  of the gait cycle during slow walking and  $21.3 \pm 1.3\%$  and  $73.4 \pm 2.6\%$  of the gait cycle during medium walking). In contrast, peaks of linear head acceleration  $V_{res}$  occurred at considerably earlier instances of the gait cycle ( $5.9 \pm 2.8\%$  and  $56.4 \pm 1.0\%$  of the gait cycle during slow walking and  $6.7 \pm 2.9\%$  and  $56.9 \pm 1.4\%$  of the gait cycle during medium walking).

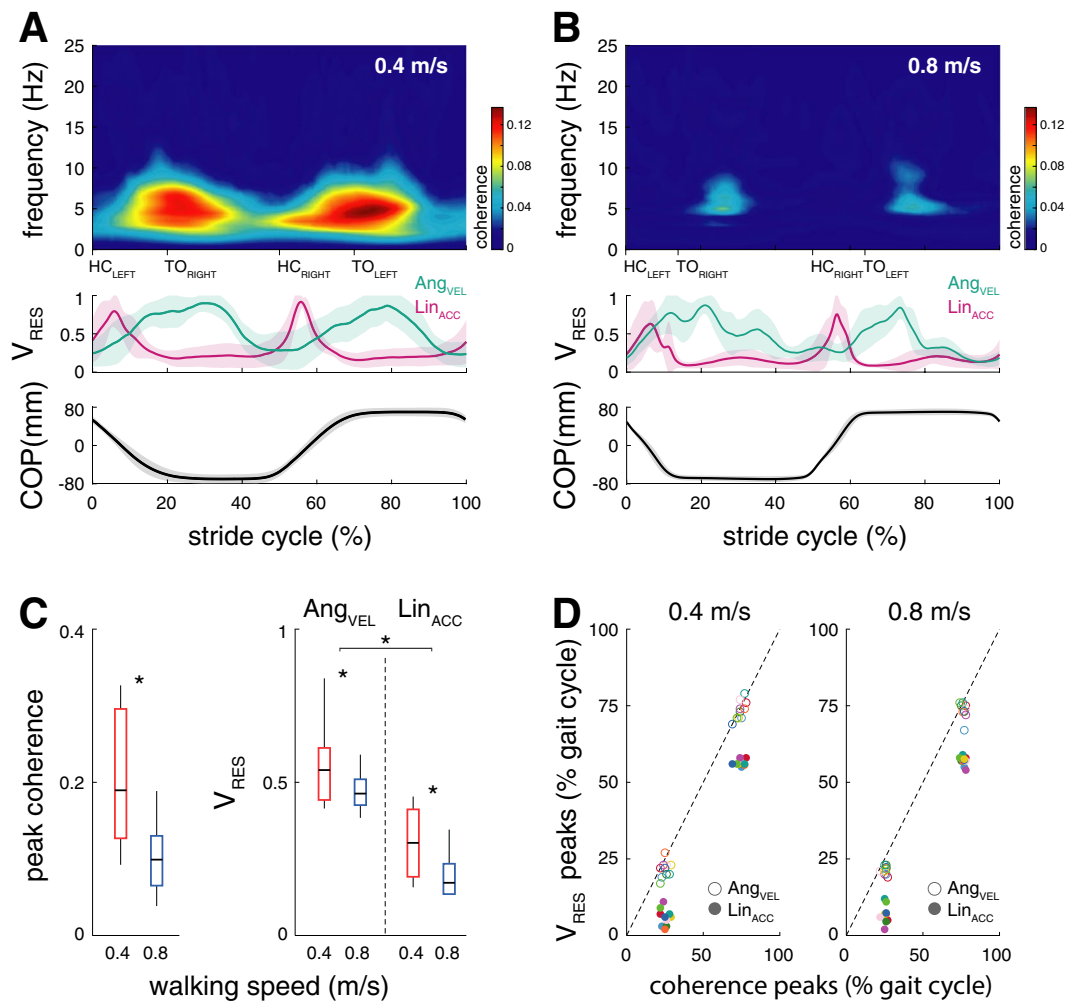


**Figure 2.** Time-frequency analysis of coupling between SVS and COP displacements and corresponding estimates of head motion predictability. **(A,B)** Average time-dependent coherence between SVS and COP at slow and medium walking speed (upper panels), corresponding average head motion  $V_{res}$  curves (middle panels), and COP motion (lower panels) in dependence on the gait cycle phase. **(C)** Peak coherence and corresponding average  $V_{res}$  for angular head velocity and linear head acceleration. **(D)** Temporal correspondence between phase-dependent peaks in SVS-COP coherence and peaks in head motion  $V_{res}$  at slow and medium walking speed. Both SVS-COP coupling and head motion predictability decrease with faster locomotion and are phase-dependently modulated across the gait cycle. SVS-COP coupling exhibits two peaks across the stride cycle that correspond well to periods of highest  $V_{res}$  (i.e., least predictability) of angular head velocity. \*Indicates a significant difference. SVS: stochastic vestibular stimulation; COP: center-of-pressure;  $V_{RES}$ : residual variance;  $Ang_{VEL}$ : angular head velocity;  $Lin_{ACC}$ : linear head acceleration; HC: heel contact; TO: toe off.

Continuous SVS did not affect the average spatiotemporal walking pattern but resulted in a considerable increase of stride-to-stride variability (i.e., increased CV) of all analyzed gait parameters (Fig. 3B). This effect was diminished during medium compared to slow walking for the CV of stride time ( $F_{1,9} = 5.9$ ;  $p = 0.038$ ), single support percentage ( $F_{1,9} = 7.7$ ;  $p = 0.022$ ), and double support percentage ( $F_{1,9} = 5.9$ ;  $p = 0.038$ ).

## Discussion

Here we observed that activity-dependent modulations of vestibular influence on balance control closely match differences in head motion predictability (HMP). This finding supports a previously proposed model<sup>12</sup>, based on the idea that during stereotyped locomotion, efference copies of locomotor commands may be used in conjunction with sensory, especially vestibular, cues in order to estimate resultant head movements and trigger adequate balance adjustments. The extent to which balance regulation during locomotion relies on concurrent vestibular vs. motor feed-forward signals should further depend on the reliability of these estimates, such that higher weighting is given to the less noisy estimate<sup>27</sup>. Accordingly, we found that activities linked to less stereotyped head movements (i.e., standing or slow walking) were more sensitive to externally triggered vestibular cues than activities with highly predictable head motion patterns (i.e., faster walking). Furthermore, we found that during walking, sensitivity to SVS was highest at the times of lowest HMP. Thus, the present results provide a reasonable explanation for the dynamic weighting of vestibular influences across and within different activities and further

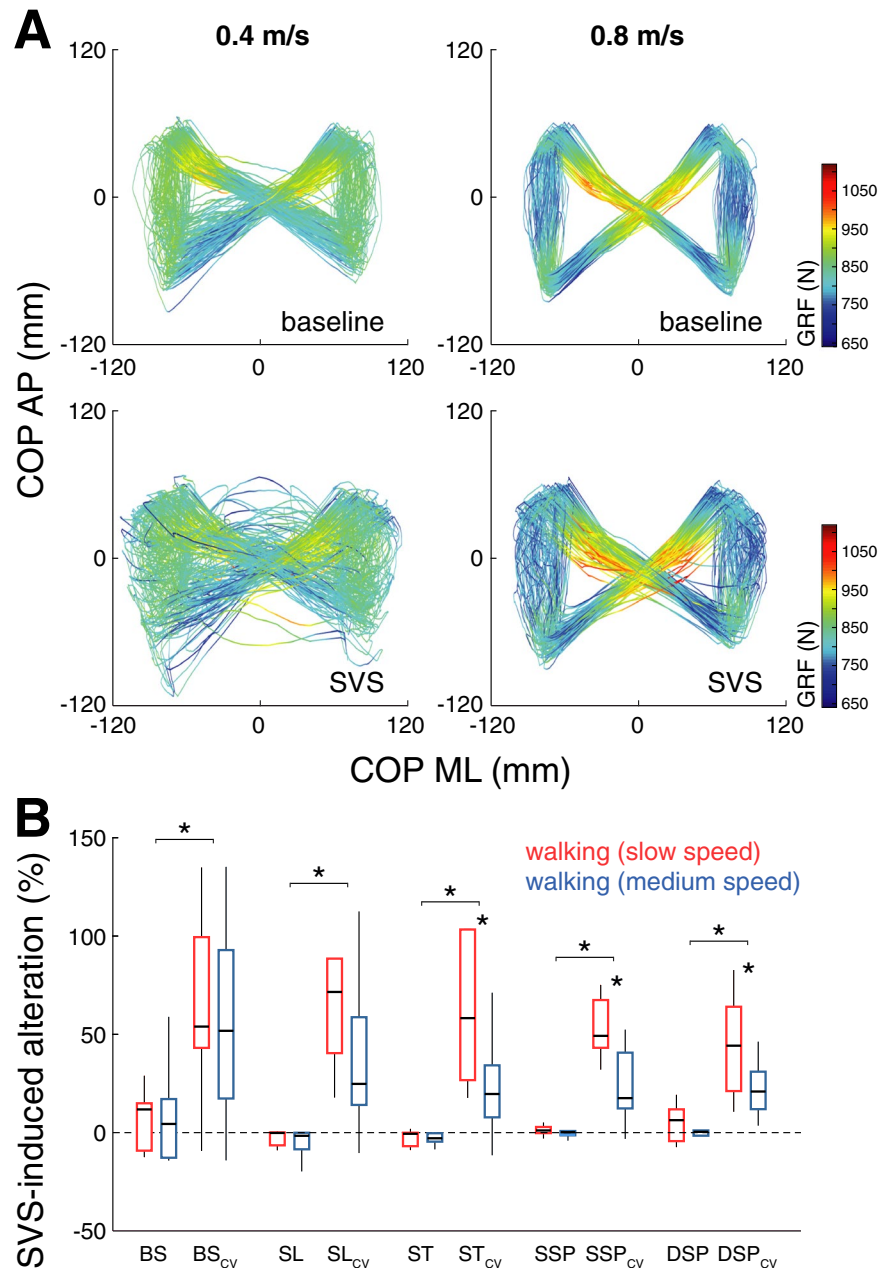


**Figure 3.** Effects of SVS and walking speed on spatiotemporal gait parameters. **(A)** Representative examples of COP trajectories during slow (left) and medium (right) walking speed for trials without stimulation (upper panel) and with continuous SVS (lower panel). **(B)** Percentage differences in gait parameters for walking with continuous SVS compared to baseline walking at the two locomotor speeds. SVS does not affect the mean gait pattern but induces increased stride-to-stride fluctuations (i.e., increased CV values) in all gait parameters. This effect diminishes with faster locomotion. \* Indicates a significant difference. SVS: *stochastic vestibular stimulation*; COP: *center-of-pressure*; BS: *base of support*; SL: *stride length*; ST: *stride time*; SSP: *single support percentage*; DSP: *double support percentage*; CV: *coefficient of variation*.

emphasize the possibility of an intrinsic feed-forward regulation of balance during human locomotion based on locomotor efference copies. In the following, we will discuss these findings with respect to their functional implications and possible physiological correlates.

The influence of externally triggered vestibular cues on body sway (i.e., SVS-COP coherence) was attenuated during walking compared to standing (Fig. 1). This agrees with the recently reported decrease of vestibular influence on body balance after gait initiation and the corresponding increase after gait termination<sup>32</sup>. Such general down-weighting of vestibular influence during locomotion is consistent with predictions of the model employed here. During locomotion, the presence of an efference copy of locomotor commands imposes an upper limit for the weighting of sensory influences, i.e.,  $w_{sens} < 1/(1+k) < 1$ , which depends on the Weber's fraction  $k$ , the proportionality constant for signal dependent noise<sup>12</sup>. Thus, balance regulation during locomotion will always be

partially governed by a locomotor efference copy, i.e.,  $w_{mot} > 0$ . Previous literature indicates that the attenuation of balance-related vestibular reflex gains during locomotion is a more general phenomenon that also concerns vestibulo-ocular reflex pathways<sup>33,34</sup>. Accordingly, it was shown in patients with a unilateral vestibular failure that spontaneous nystagmus resulting from a vestibular tone imbalance is considerably dampened during ambulation<sup>35</sup>. A complete suppression of the horizontal vestibulo-ocular reflex has been demonstrated in tadpole swimming, i.e., a locomotor activity where the spatiotemporal coupling between rhythmic propulsive locomotor movements and resultant head displacements is high<sup>10,16</sup>. Similar effects were also observed in other non-vestibular sensory modalities. For instance, proprioceptive stretch reflexes that govern postural control during standing are known to be selectively suppressed during locomotion<sup>36</sup>. This does not mean that static postural control is purely governed by sensory feedback regulation. Feed-forward postural adjustments are well documented for both voluntary self-initiated and predictable external balance perturbations<sup>37</sup>. However, it is still controversially discussed whether and to what extent feed-forward control also governs static undisturbed balance regulation<sup>38</sup>.

During locomotion, vestibular feedback is thought to be essential for the maintenance of dynamic stability by fine-tuning the timing and magnitude of foot placement<sup>2,4,8</sup>. In line with this, significant SVS-COP coupling during locomotion led to an increased spatiotemporal variability of stride-to-stride walking movements despite the otherwise unaffected average gait parameters (Fig. 3). Both SVS-COP coupling and increased stride-to-stride variability decreased from slow to medium walking speed (Figs. 1–3). This observation is in line with previous studies reporting that the destabilizing impact of a vestibular loss or external vestibular perturbation becomes considerably attenuated with increased locomotor velocity and cadence<sup>3,5,7,9</sup>. Moreover, we found that SVS-COP coupling was phase-dependently modulated during locomotion, exhibiting two consistent peaks across the gait cycle with equal timing for both examined walking speeds. Both speed- and phase-dependent changes in SVS-COP coupling closely matched concomitant changes in HMP (Fig. 2). Accordingly,  $V_{res}$  of linear acceleration and angular velocity of head motion decreased with faster locomotion (i.e., increased predictability) and consistently exhibited two local maxima across the gait cycle (i.e., least predictability). These phase-dependent changes of HMP in the ML dimension show a substantial temporal agreement with previously reported modulations of vestibulo-muscular coupling across the locomotor cycle, in particular for muscle groups that mediate ML body sway<sup>2,3</sup>. It is yet unclear, whether the coincidence between modulations in SVS-COP coupling and HMP observed during symmetric steady-state walking continues to exist during asymmetric walking modes (e.g., split-belt walking or walking along a curved path), where vestibulo-muscular coupling has been shown to be independently modulated in each limb<sup>39</sup>. Finally, phasic modulation of SVS-COP coupling across the locomotor cycle temporally matched modulations of  $V_{res}$  of angular head velocity rather than of linear head acceleration. This suggests that the observed SVS-induced COP displacements primarily reflect responses to activation of semicircular canal afferents. In line with this, medium-latency body sway responses at the frequency bandwidth and phase lags observed in the present study were previously shown to most likely reflect semicircular canal afferent responses to galvanic vestibular stimulation<sup>40,41</sup>.

Previous reports hypothesized that the activity-dependent modulation of vestibular feedback during locomotion is reflected by concurrent changes in muscle activation or foot placement patterns to stabilize posture<sup>2–4</sup>. Others have proposed that vestibular down-regulation during faster locomotion simply occurs due to a larger degree of automated behavior<sup>5</sup> or biomechanical stability<sup>32</sup> that tends to rely less on sensory feedback. Besides, the rapid stepping patterns at faster locomotion might impose too short time frames for an adequate operation of vestibular balance reflexes with latencies of about 50–60 ms<sup>42</sup>. However, even at fast running with gait cycle durations of about 600 ms<sup>43</sup>, vestibulospinal reflexes should be fast enough to efficiently stabilize posture. The present findings suggest that, besides automation, stability, or time-constraints, changes in HMP play an important role in defining the activity-dependent modulation of vestibular control of balance during locomotion. Accordingly, despite the increase of sensory and motor noise linked to faster movements<sup>28,29,44</sup> the relative ratio of sensory vs. motor noise does not remain constant but appears to become greater with increasing locomotion speed. The relative increase in sensory noise should lead to a down-weighting of vestibular feedback in favor of a direct feed-forward control of balance based on efference copies from the locomotor commands. Moreover, the phase-dependent modulation of vestibular influences would similarly reflect changes in the proportion of sensory vs. motor noise across the gait cycle. An analogous re-weighting of sensory vs. motor cues based on the relative precision of these signals could further explain the previously described speed- and phase-dependent modulation of other non-vestibular feedback cues (i.e., visual and proprioceptive) during human locomotion<sup>45–49</sup>.

The relationship between the activity-dependent modulation of vestibular influences and changes in HMP suggests that during human locomotion an intrinsic feed-forward mechanism based on locomotor efference copies plays a significant part in balance regulation, which was previously thought to be predominantly governed by sensorimotor reflexes. Traditionally, motor efference copies are primarily considered to serve as predictors of sensory consequences arising from one's own actions, thereby enabling the brain to distinguish self-generated sensory signals (reafference) from sensory inputs caused by unpredictable external influences (exafference)<sup>50–52</sup>. Recent research, however, has expanded this view, suggesting that internal motor predictions are also involved in coordinating action of different motor systems that are otherwise functionally and anatomically unrelated<sup>14</sup>. One well described example of such an efference copy-mediated motor-to-motor coupling is the interaction between the mammalian locomotor and respiratory motor system, which is coordinated by intrinsic efference copies derived from CPG activity in the lumbar spinal cord<sup>53</sup>. More recently, CPG-derived locomotor efference copies were shown to directly mediate compensatory eye movements for gaze stabilization during aquatic locomotion in *Xenopus laevis* tadpoles<sup>10</sup> and adult frogs<sup>15</sup> – a task that is usually thought to be mediated by the vestibulo-ocular reflex. Importantly, the direct coupling between spinal and ocular motor signals was shown to be accompanied by a selective suppression of both ex- and reafferent vestibular inputs to extraocular motoneurons. Moreover, the

activity-dependent suppression was proven to be plane-specific and only interfered with vestibular inputs related to the primary plane of head movements during aquatic locomotion. Whether such a selective and plane-specific gating of total vestibular inflow occurs at the level of the brainstem extraocular or vestibular nuclei or other brain regions such as the cerebellum yet remains unknown. In favor of a cerebellar origin, it was previously shown that the phasic modulation of vestibulospinal neuron activity in the lateral vestibular nucleus observed during locomotion in cats depends on the presence of an intact cerebellum and is disrupted by its removal<sup>54,55</sup>. Given its prominent role in adaptive plasticity of vestibular reflexes<sup>1,56,57</sup>, the cerebellum might thus serve as a convergence site for the weighting and integration of self-motion derived vestibular cues and intrinsic locomotor efference copies.

### Data availability

The datasets generated and analyzed during the current study are available from the corresponding author on reasonable request.

Received: 8 May 2019; Accepted: 21 December 2019;

Published online: 20 January 2020

### References

- Angelaki, D. E. & Cullen, K. E. Vestibular system: the many facets of a multimodal sense. *Annu. Rev. Neurosci.* **31**, 125–150, <https://doi.org/10.1146/annurev.neuro.31.060407.125555> (2008).
- Blouin, J. S. *et al.* Extracting phase-dependent human vestibular reflexes during locomotion using both time and frequency correlation approaches. *J. Appl. Physiol.* **111**, 1484–1490, <https://doi.org/10.1152/jappphysiol.00621.2011> (2011).
- Dakin, C. J., Inglis, J. T., Chua, R. & Blouin, J. S. Muscle-specific modulation of vestibular reflexes with increased locomotor velocity and cadence. *J. Neurophysiol.* **110**, 86–94, <https://doi.org/10.1152/jn.00843.2012> (2013).
- Bent, L. R., Inglis, J. T. & McFadyen, B. J. When is vestibular information important during walking? *J. Neurophysiol.* **92**, 1269–1275 (2004).
- Brandt, T., Strupp, M. & Benson, J. You are better off running than walking with acute vestibulopathy. *Lancet* **354**, 746, [https://doi.org/10.1016/S0140-6736\(99\)03179-7](https://doi.org/10.1016/S0140-6736(99)03179-7) (1999).
- Schniepp, R. *et al.* Clinical and neurophysiological risk factors for falls in patients with bilateral vestibulopathy. *J. Neurol.* **264**, 277–283, <https://doi.org/10.1007/s00415-016-8342-6> (2017).
- Schniepp, R. *et al.* Locomotion speed determines gait variability in cerebellar ataxia and vestibular failure. *Mov. Disord.* **27**, 125–131, <https://doi.org/10.1002/mds.23978> (2012).
- Wuehr, M. *et al.* Noisy vestibular stimulation improves dynamic walking stability in bilateral vestibulopathy. *Neurology* **86**, 2196–2202, <https://doi.org/10.1212/WNL.0000000000002748> (2016).
- Jahn, K., Strupp, M., Schneider, E., Dieterich, M. & Brandt, T. Differential effects of vestibular stimulation on walking and running. *Neuroreport* **11**, 1745–1748 (2000).
- Lambert, F. M., Combes, D., Simmers, J. & Straka, H. Gaze stabilization by efference copy signaling without sensory feedback during vertebrate locomotion. *Curr. Biol.* **22**, 1649–1658, <https://doi.org/10.1016/j.cub.2012.07.019> (2012).
- Roy, J. E. & Cullen, K. E. Dissociating self-generated from passively applied head motion: neural mechanisms in the vestibular nuclei. *J. Neurosci.* **24**, 2102–2111, <https://doi.org/10.1523/JNEUROSCI.3988-03.2004> (2004).
- MacNeilage, P. R. & Glasauer, S. Quantification of Head Movement Predictability and Implications for Suppression of Vestibular Input during Locomotion. *Front. Comput. Neurosci.* **11**, 47, <https://doi.org/10.3389/fncom.2017.00047> (2017).
- Sağlam, M., Glasauer, S. & Lehnen, N. Vestibular and cerebellar contribution to gaze optimality. *Brain* **137**, 1080–1094, <https://doi.org/10.1093/brain/awu006> (2014).
- Straka, H., Simmers, J. & Chagnaud, B. P. A New Perspective on Predictive Motor Signaling. *Curr. Biol.* **28**, R232–R243, <https://doi.org/10.1016/j.cub.2018.01.033> (2018).
- von Uckermann, G., Le Ray, D., Combes, D., Straka, H. & Simmers, J. Spinal efference copy signaling and gaze stabilization during locomotion in juvenile *Xenopus* frogs. *J. Neurosci.* **33**, 4253–4264, <https://doi.org/10.1523/JNEUROSCI.4521-12.2013> (2013).
- Chagnaud, B. P., Simmers, J. & Straka, H. Predictability of visual perturbation during locomotion: implications for corrective efference copy signaling. *Biol. Cybern.* **106**, 669–679, <https://doi.org/10.1007/s00422-012-0528-0> (2012).
- Kwan, A., Forbes, P. A., Mitchell, D. E., Blouin, J.-S. & Cullen, K. E. Neural substrates, dynamics and thresholds of galvanic vestibular stimulation in the behaving primate. *Nat. Commun.* **10**, 1904, <https://doi.org/10.1038/s41467-019-09738-1> (2019).
- Goldberg, J., Smith, C. E. & Fernandez, C. Relation between discharge regularity and responses to externally applied galvanic currents in vestibular nerve afferents of the squirrel monkey. *J. Neurophysiol.* **51**, 1236–1256 (1984).
- Kim, J. & Curthoys, I. S. Responses of primary vestibular neurons to galvanic vestibular stimulation (GVS) in the anaesthetized guinea pig. *Brain Res. Bull.* **64**, 265–271, <https://doi.org/10.1016/j.brainresbull.2004.07.008> (2004).
- Fitzpatrick, R. C. & Day, B. L. Probing the human vestibular system with galvanic stimulation. *J. Appl. Physiol.* **96**, 2301–2316, <https://doi.org/10.1152/jappphysiol.00008.2004> (2004).
- Schneider, E., Glasauer, S. & Dieterich, M. Comparison of human ocular torsion patterns during natural and galvanic vestibular stimulation. *J. Neurophysiol.* **87**, 2064–2073, <https://doi.org/10.1152/jn.00558.2001> (2002).
- Iles, J. F., Baderin, R., Tanner, R. & Simon, A. Human standing and walking: comparison of the effects of stimulation of the vestibular system. *Exp. Brain Res.* **178**, 151–166, <https://doi.org/10.1007/s00221-006-0721-2> (2007).
- Terrier, P. & Deriaz, O. Non-linear dynamics of human locomotion: effects of rhythmic auditory cueing on local dynamic stability. *Front. Physiol.* **4**, 230, <https://doi.org/10.3389/fphys.2013.00230> (2013).
- Rosenberg, J., Amjad, A., Breeze, P., Brillinger, D. & Halliday, D. The Fourier approach to the identification of functional coupling between neuronal spike trains. *Prog. Biophys. Mol. Biol.* **53**, 1–31 (1989).
- Dakin, C. J., Son, G. M., Inglis, J. T. & Blouin, J. S. Frequency response of human vestibular reflexes characterized by stochastic stimuli. *J. Physiol.* **583**, 1117–1127, <https://doi.org/10.1113/jphysiol.2007.133264> (2007).
- Zhan, Y., Halliday, D., Jiang, P., Liu, X. & Feng, J. Detecting time-dependent coherence between non-stationary electrophysiological signals—a combined statistical and time-frequency approach. *J. Neurosci. Methods* **156**, 322–332, <https://doi.org/10.1016/j.jneumeth.2006.02.013> (2006).
- Ernst, M. O. & Banks, M. S. Humans integrate visual and haptic information in a statistically optimal fashion. *Nature* **415**, 429–433, <https://doi.org/10.1038/415429a> (2002).
- Fechner, G. T. *Elemente der Psychophysik*. (Breitkopf und Härtel, 1860).
- Harris, C. M. & Wolpert, D. M. Signal-dependent noise determines motor planning. *Nature* **394**, 780–784, <https://doi.org/10.1038/29528> (1998).
- Jones, K. E., Hamilton, A. F. C. & Wolpert, D. M. Sources of Signal-Dependent Noise During Isometric Force Production. *J. Neurophysiol.* **88**, 1533–1544, <https://doi.org/10.1152/jn.2002.88.3.1533> (2002).



31. Fitts, P. M. The information capacity of the human motor system in controlling the amplitude of movement. *J. Exp. Psychol.* **47**, 381–391 (1954).
32. Tisserand, R. *et al.* Down regulation of vestibular balance stabilizing mechanisms to enable transition between motor states. *eLife* **7** (2018).
33. Dietrich, H. & Wuehr, M. Strategies for Gaze Stabilization Critically Depend on Locomotor Speed. *Neuroscience* **408**, 418–429, <https://doi.org/10.1016/j.neuroscience.2019.01.025> (2019).
34. Dietrich, H. & Wuehr, M. Selective suppression of the vestibulo-ocular reflex during human locomotion. *J. Neurol.* **266**, 101–107, <https://doi.org/10.1007/s00415-019-09352-7> (2019).
35. Jahn, K., Strupp, M. & Brandt, T. Both actual and imagined locomotion suppress spontaneous vestibular nystagmus. *Neuroreport* **13**, 2125–2128 (2002).
36. Dietz, V., Quintern, J. & Berger, W. Afferent control of human stance and gait: evidence for blocking of group I afferents during gait. *Exp. Brain Res.* **61**, 153–163 (1985).
37. Massion, J. Postural control system. *Curr. Opin. Neurobiol.* **4**, 877–887 (1994).
38. Forbes, P. A., Chen, A. & Blouin, J.-S. In *Handbook of Clinical Neurology* Vol. 159 (eds Brian L. Day & Stephen R. Lord) 61–83 (Elsevier, 2018).
39. Forbes, P. A. *et al.* Rapid limb-specific modulation of vestibular contributions to ankle muscle activity during locomotion. *J. Physiol.* **595**, 2175–2195, <https://doi.org/10.1113/jp272614> (2017).
40. Cathers, L., Day, B. L. & Fitzpatrick, R. C. Otolith and canal reflexes in human standing. *J. Physiol.* **563**, 229–234, <https://doi.org/10.1113/jphysiol.2004.079525> (2005).
41. Mian, O. S., Dakin, C. J., Blouin, J.-S., Fitzpatrick, R. C. & Day, B. L. Lack of otolith involvement in balance responses evoked by mastoid electrical stimulation. *J. Physiol.* **588**, 4441–4451, <https://doi.org/10.1113/jphysiol.2010.195222> (2010).
42. Britton, T. C. *et al.* Postural electromyographic responses in the arm and leg following galvanic vestibular stimulation in man. *Exp. Brain Res.* **94**, 143–151, <https://doi.org/10.1007/bf00230477> (1993).
43. Nilsson, J., Thorstensson, A. & Halbertsma, J. Changes in leg movements and muscle activity with speed of locomotion and mode of progression in humans. *Acta Physiol. Scand.* **123**, 457–475, <https://doi.org/10.1111/j.1748-1716.1985.tb07612.x> (1985).
44. Faisal, A. A., Selen, L. P. & Wolpert, D. M. Noise in the nervous system. *Nat. Rev. Neurosci.* **9**, 292–303, <https://doi.org/10.1038/nrn2258> (2008).
45. Wuehr, M. *et al.* Sensory loss and walking speed related factors for gait alterations in patients with peripheral neuropathy. *Gait Posture* **39**, 852–858, <https://doi.org/10.1016/j.gaitpost.2013.11.013> (2014).
46. Wuehr, M. *et al.* Differential effects of absent visual feedback control on gait variability during different locomotion speeds. *Exp. Brain Res.* **224**, 287–294, <https://doi.org/10.1007/s00221-012-3310-6> (2013).
47. Jahn, K., Strupp, M., Schneider, E., Dieterich, M. & Brandt, T. Visually induced gait deviations during different locomotion speeds. *Exp. Brain Res.* **141**, 370–374, <https://doi.org/10.1007/s002210100884> (2001).
48. Dietz, V. Proprioception and locomotor disorders. *Nat. Rev. Neurosci.* **3**, 781–790, <https://doi.org/10.1038/nrn939> (2002).
49. Logan, D. *et al.* Function dictates the phase dependence of vision during human locomotion. *J. Neurophysiol.* **112**, 165–180, <https://doi.org/10.1152/jn.01062.2012> (2014).
50. von Holst, E. & Mittelstaedt, H. Das Reafferenzprinzip. Wechselwirkungen zwischen Zentralnervensystem und Peripherie. *Die Naturwissenschaften* **37**, 464–476 (1950).
51. Sperry, R. W. Neural basis of the spontaneous optokinetic response produced by visual inversion. *J. Comp. Physiol. Psychol.* **43**, 482–489 (1950).
52. Cullen, K. E. Sensory signals during active versus passive movement. *Curr. Opin. Neurobiol.* **14**, 698–706, <https://doi.org/10.1016/j.conb.2004.10.002> (2004).
53. Onimaru, H. & Homma, I. A novel functional neuron group for respiratory rhythm generation in the ventral medulla. *J. Neurosci.* **23**, 1478–1486 (2003).
54. Orlovsky, G. N. Activity of vestibulospinal neurons during locomotion. *Brain Res.* **46**, 85–98 (1972).
55. Udo, M., Kamei, H., Matsukawa, K. & Tanaka, K. Interlimb coordination in cat locomotion investigated with perturbation. II. Correlates in neuronal activity of Deiter's cells of decerebrate walking cats. *Exp. Brain Res.* **46**, 438–447 (1982).
56. Gittis, A. H. & du Lac, S. Intrinsic and synaptic plasticity in the vestibular system. *Curr. Opin. Neurobiol.* **16**, 385–390 (2006).
57. Dietrich, H. & Straka, H. Prolonged vestibular stimulation induces homeostatic plasticity of the vestibulo-ocular reflex in larval *Xenopus laevis*. *Eur. J. Neurosci.* **44**, 1787–1796, <https://doi.org/10.1111/ejn.13269> (2016).

## Acknowledgements

This work was supported by the German Federal Ministry of Education and Research (01EO1401) and the German Research Foundation (MA 6233/1-1).

## Author contributions

All of the authors have taken part in the preparation of this manuscript, have reviewed the results, and have approved the final version of this manuscript. H.D., R.S., S.G. and M.W. conceptualized and designed the study. H.D., F.H., R.S., P.R.M., S.G. and M.W. collected, analyzed, and interpreted the data. H.D. and M.W. wrote the paper.

## Competing interests

The authors declare no competing interest.

## Additional information

**Correspondence** and requests for materials should be addressed to M.W.

**Reprints and permissions information** is available at [www.nature.com/reprints](http://www.nature.com/reprints).

**Publisher's note** Springer Nature remains neutral with regard to jurisdictional claims in published maps and institutional affiliations.



**Open Access** This article is licensed under a Creative Commons Attribution 4.0 International License, which permits use, sharing, adaptation, distribution and reproduction in any medium or format, as long as you give appropriate credit to the original author(s) and the source, provide a link to the Creative Commons license, and indicate if changes were made. The images or other third party material in this article are included in the article's Creative Commons license, unless indicated otherwise in a credit line to the material. If material is not included in the article's Creative Commons license and your intended use is not permitted by statutory regulation or exceeds the permitted use, you will need to obtain permission directly from the copyright holder. To view a copy of this license, visit <http://creativecommons.org/licenses/by/4.0/>.

© The Author(s) 2020